Title

Seismic compression of two compacted earth fills shaken by the 1994 northridge earthquake

Journal

Journal of Geotechnical and Geoenvironmental Engineering, 130(5)

ISSN

1090-0241

Authors

Stewart, Jonathan P
Smith, Patrick M
Whang, Daniel H
et al.

Publication Date

2004-05-01

Peer reviewed

Seismic Compression of Two Compacted Earth Fills Shaken by the 1994 Northridge Earthquake

Jonathan P. Stewart, M.ASCE[1]; Patrick M. Smith, A.M.ASCE[2]; Daniel H. Whang, A.M.ASCE[3]; and Jonathan D. Bray, M.ASCE[4]

Abstract: Seismic compression is defined as the accrual of contractive volumetric strain in unsaturated soil during strong shaking by earthquakes. We document and analyze two case histories (denoted school site and site A) of ground deformation from seismic compression in canyon fills strongly shaken by the Northridge earthquake. Site A had ground settlements up to about 18 cm, which damaged a structure, while the school site had settlements up to about 6 cm. For each site, we perform decoupled analyses of shear and volumetric strain. Shear strain is calculated using one-dimensional and two-dimensional ground response analyses, while volumetric strain is evaluated from shear strain using material-specific models derived from simple shear laboratory testing that incorporates important effects of fines content and as-compacted density and saturation. Analyses are repeated using a logic tree approach in which weights are assigned to multiple possible realizations of uncertain model parameters. At the school site, predicted settlements appear to be unbiased. At site A, the analyses successfully predict the shape of the settlement profile along a section, but the weighted average predictions are biased slightly too low. We speculate that the apparent site A bias can be explained by limited resolution of the site stratigraphy, bias in laboratory-derived volumetric strain models, and/or uncertainty in the estimated earthquake-induced settlements.

DOI: 10.1061/(ASCE)1090-0241(2004)130:5(461)

CE Database subject headings: Compression; Seismic effects; Earthquakes; Shear strain; California.

Introduction

Seismic compression is defined as the accrual of contractive volumetric strain in unsaturated soil during strong shaking by earthquakes. Ground deformation in compacted fill materials from seismic compression has been documented in earlier literature. However, previously reported case histories typically consists of (1) hillside fill slopes, where the general nature of ground deformation is reported, but absolute ground displacement is not known due to a lack of available pre-earthquake fill position surveys (see, e.g., Seed 1967; Pyke et al. 1975; Slosson 1975; Stewart et al. 2001) and (2) fills adjacent to bridge abutment walls, where relative settlements are available, but the case histories typically involve uncompacted or poorly compacted fill for which little information is available on soil type or compaction conditions (Siddharthan and El-Gamal 1996). The paucity of high quality case histories with measured ground displacements and well-characterized soil conditions represents a significant hindrance to the calibration of seismic compression analysis procedures.

To the writers' knowledge, the only previously well-documented case history of ground displacement from seismic compression is from the Jensen Filtration Plant site during the 1971 San Fernando earthquake, reported by Pyke et al. (1975). A 17-m thick fill blanket with well-documented compaction conditions was reported to have experienced settlement and lateral ground displacements along a survey baseline of about 13 cm. However, these displacements occurred on a section of fill that underwent lateral spreading as a result of liquefaction of underlying alluvium, which opened a ground crack near the survey baseline. Accordingly, Pyke et al. could only estimate the fraction of overall settlement due to seismic compression. Even this lone case history of seismic compression-induced settlement should be interpreted with caution.

In this paper, we document and analyze two case histories (denoted school site and site A) where ground displacements from seismic compression are known or can be accurately estimated from pre- and postearthquake surveys. Both case studies involve deep canyon fills in Santa Clarita, California, an area strongly shaken by the Northridge earthquake (peak ground accelerations on rock $\approx 0.3-0.7g$). The seismic performance of the fills was quite different. Site A had ground settlements up to $\sim$18 cm, which damaged a structure, whereas the school site had measured settlements $\leqslant$6.1 cm. The analyses performed for these sites have two principal objectives: (1) to investigate the degree to which seismic compression can explain the observed ground displacements and (2) to evaluate the sensitivity of calculated settlements to variability in input parameters as well as dispersion of calculated settlements given the overall parametric variability. The analysis procedure consists of ground response calculations to evaluate shear strains in the fill mass, which are then coupled with

[1]Associate Professor, Civil and Environmental Engineering Dept., 5731 Boelter Hall, Univ. of California, Los Angeles, CA 90095. E-mail: jstewart@seas.ucla.edu

[2]Project Engineer, Praad Geotechnical, 5465 South Centinela Ave., Los Angeles, CA 90066.

[3]Assistant Research Engineer, Civil and Environmental Engineering Dept., 6679 Boelter Hall, Univ. of California, Los Angeles, CA 90095.

[4]Professor, Civil and Environmental Engineering Dept., 440 Davis Hall, Univ. of California, Berkeley, CA 94720.

Note. Discussion open until October 1, 2004. Separate discussions must be submitted for individual papers. To extend the closing date by one month, a written request must be filed with the ASCE Managing Editor. The manuscript for this paper was submitted for review and possible publication on January 13, 2003; approved on July 28, 2003. This paper is part of the ***Journal of Geotechnical and Geoenvironmental Engineering***, Vol. 130, No. 5, May 1, 2004. ©ASCE, ISSN 1090-0241/2004/5-461–476/$18.00.

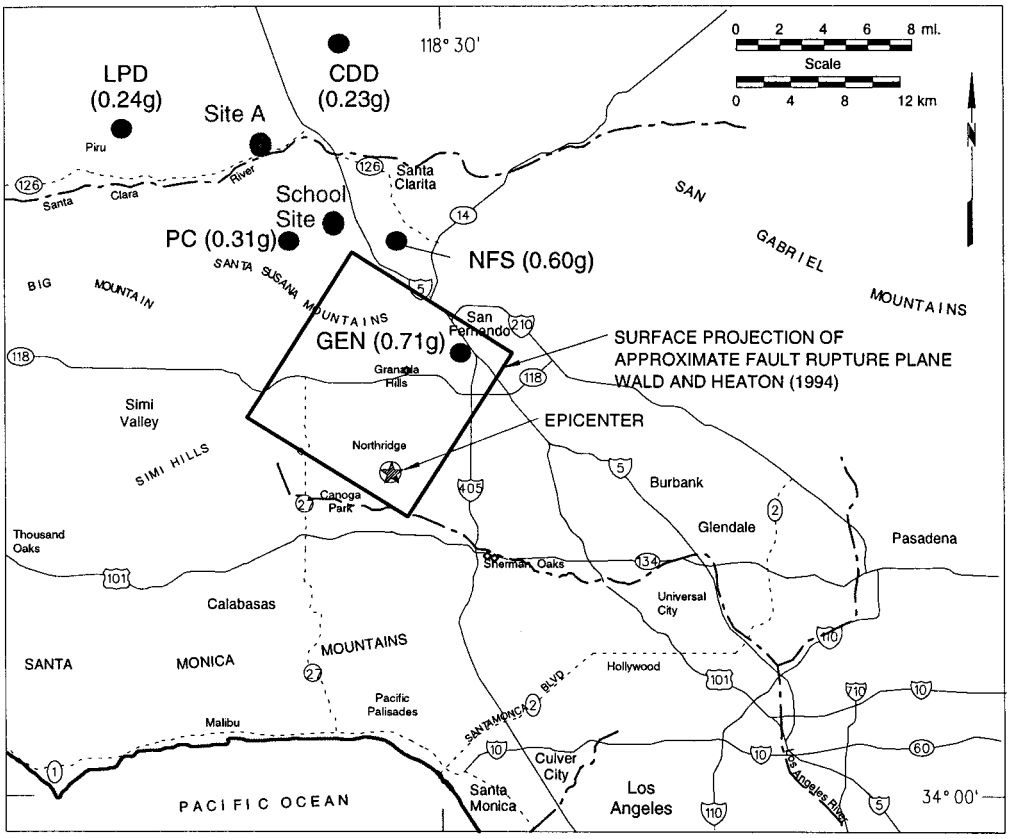

Fig. 1. Locations of school site and site A and selected strong motion stations (with geometric mean peak horizontal accelerations from 1994 Northridge earthquake in parentheses)

material-specific relationships between shear and volumetric strain derived from simple shear laboratory testing. The volumetric strains are integrated over the fill thickness to estimate settlement. It should be noted that the relatively simplified method of seismic compression analysis proposed by Tokimatsu and Seed (1987) is not appropriate for analysis of the present sites because the method was developed for clean sand and the soils at the subject sites contain significant fines. Nonetheless, that procedure represents the current state of practice (even for fine-grained soil), and hence we briefly compare the predictions of that method to the data as well.

This paper is organized into sections which: (1) Document the geotechnical site conditions (including laboratory test results) and observed field performance during the Northridge earthquake, (2) describe the ground shaking characteristics expected at the two sites from local recordings, and (3) describe the results of the aforementioned analyses, including comparisons of analysis results to data and sensitivity studies.

Site Conditions and Field Performance

School Site

As shown in Fig. 1, the school site is located in the Santa Clarita Valley, and is about 7.2 km from the Northridge earthquake fault rupture plane. A plan view and cross section of the 9,310 m^2 site are shown in Figs. 2 and 3, respectively. The original topography at the site consisted of several steeply sloping canyons, with a general increase in elevation to the west and north. The fill was constructed in October and November of 1993, and involved cuts into the hillside at the west and north ends of the site, and deep fills extending to depths of up to 30.5 m at the east and south ends. All cut areas were overexcavated to maintain a minimum depth of fill of about 15 m under the planned building location.

One rotary wash boring was drilled at the site at the location shown in Fig. 2, which extended through the fill and approximately 33.5 m into bedrock. Suspension logging was performed in the borehole to measure seismic velocities. Three seismic cone penetration tests (SCPTs) were also performed in the fill at the locations shown in Fig. 2. As illustrated by the boring log in Fig. 4, the fill soils consist of sandy silt and silty sand and occasional gravel. The fines contents in the fill range from 43 to 61% (average=52%), and results of Atterberg limit tests generally plot below the "A" line [average liquid limit (LL)=28 and plasticity index (PI)=5], providing ML or SM soil classifications by the Unified Soil Classification System (although some SC materials are also present). The fill is underlain by interbedded weathered sandstone and conglomerate that belong to the Saugas Formation. Ground water was not encountered in any of the SCPTs or in the boring.

To minimize potential settlement due to hydrocompression, fill placed at the site was required to have as-compacted water contents greater than the optimum water content (w_{opt}) based on the modified Proctor standard in ASTM D1557 (ASTM 2002). In addition, dual density criteria were employed. The first criterion applied to fill supporting structures and consisted of a minimum relative compaction (RC) (=dry density/maximum dry density

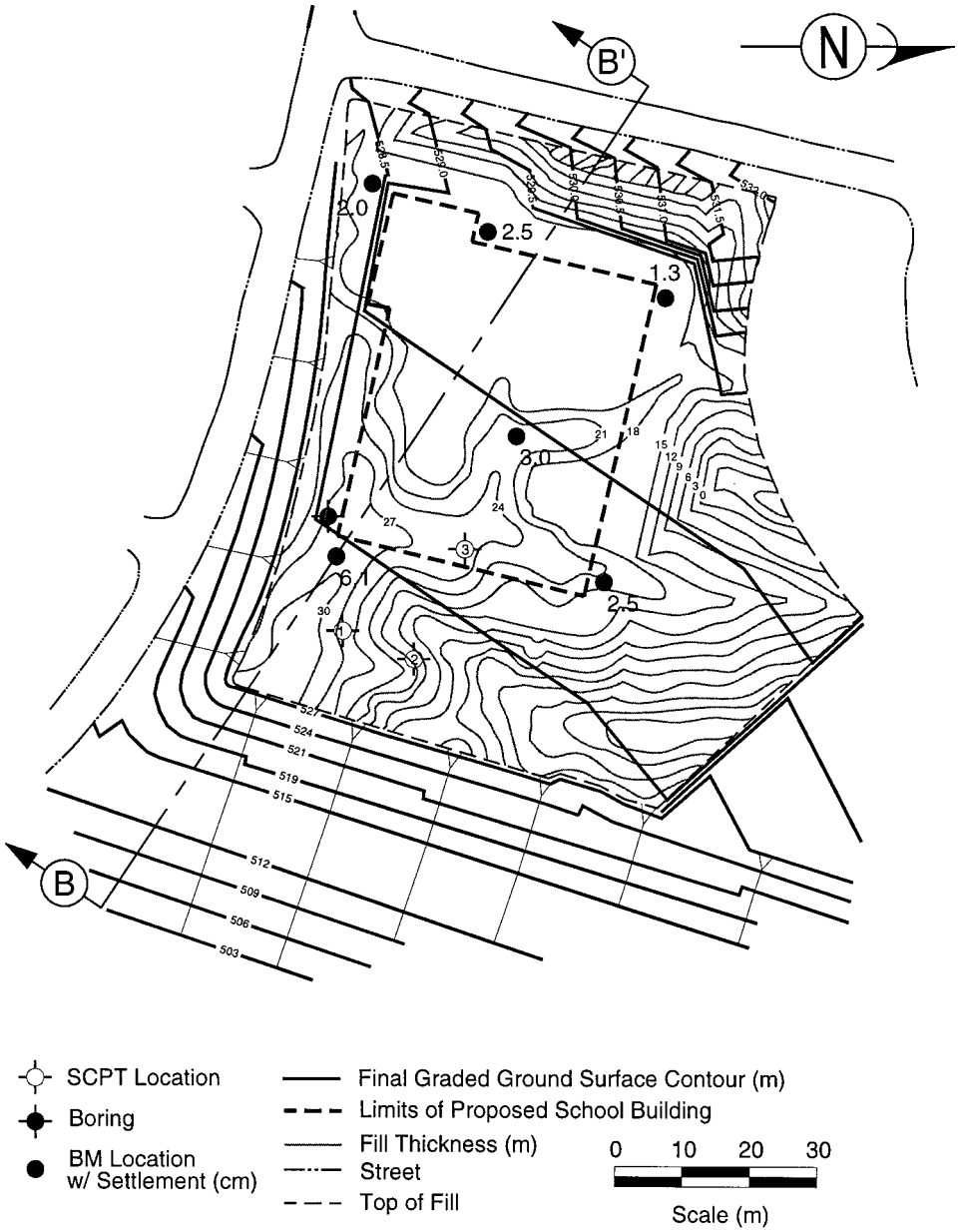

Fig. 2. School site plan view showing depth-of-fill contours, locations of subsurface exploration, and locations of fill settlement benchmarks

from the compaction curve) by modified Proctor standard of 95% (95% RC) at fill depths >3 m, while the second criterion applied to fills in the upper 3 m and to open space areas and consisted of a minimum of 90% RC. All fill materials at depths >15 m were subject to the 95% RC standard, and transitions from the 95 to 90% zones were accomplished with a 2H:1V slope across the top of the 95% zone.

We developed compaction curves for five specimens retrieved from the site (four from borehole samples and one from a test pit bulk sample), the results of which are consistent with those obtained at the time of construction by the consulting engineer. Accordingly, 1,180 field compaction tests by the project consultant were used as an initial estimate of the RC and w values of the as-compacted fill. These data were compiled by discretizing the RC space into 1% intervals and the w space into 1% intervals, and then calculating the percentage of all tests within each of those bins. As described by Stewart et al. (2002), the resulting distributions of RC in the 90 and 95% zones were truncated at their respective minimum RC values, which we judged to be unrealistic. Accordingly, we used the Kriging geostatistical gridding method (Cressie 1991) to infer a distribution below the truncation limit. The Kriging gridding method essentially performs this extrapolation based on trends of the data at higher RC. The contoured likelihoods across RC–w space are shown in Fig. 5 along with standard and modified Proctor moisture-density curves and contour lines for a constant degree of saturation based on $G_s = 2.70$. The modes of the original and modified data sets are similar, ~93% RC in the 90% RC zone and ~95% RC in the 95% RC zone. Fill in the 90% RC zone spans the line of optima, whereas fill in the 95% RC zone is generally wet of the line of optima.

Simple shear laboratory testing was performed to evaluate the seismic compression potential of three soil samples from the school site (samples B-1–B-3). These soils are silty or clayey sand (either SM or SC), with 40–48% fines and PI$=2-14$. Of the three samples, B-3 is the most representative of field conditions

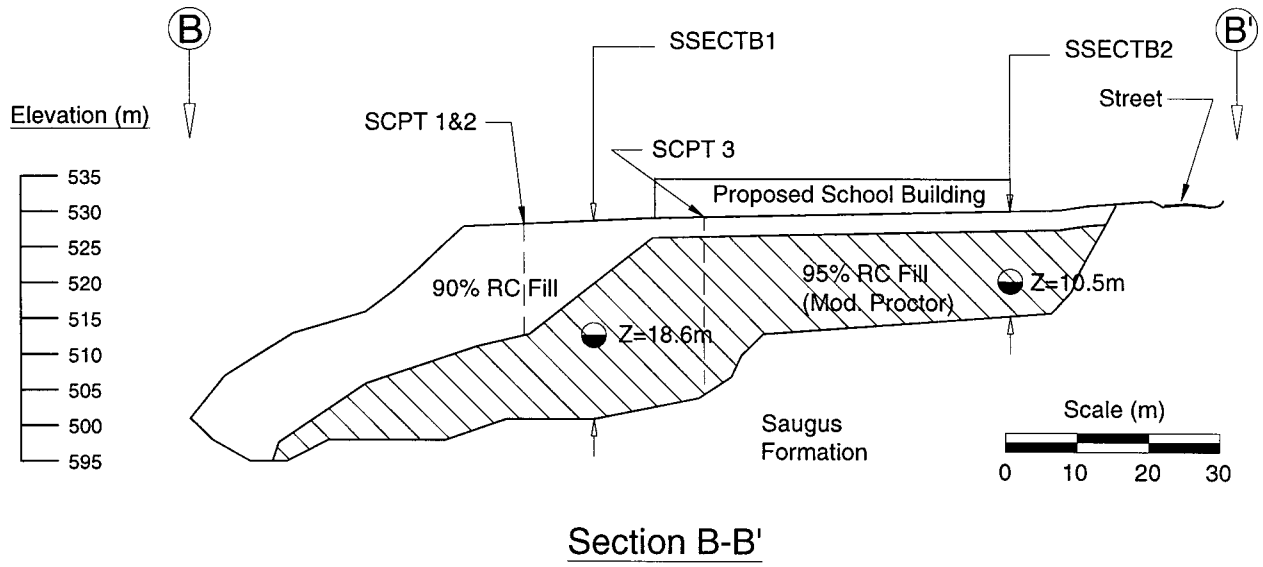

Fig. 3. Cross section B–B′ at school site showing locations of vertical profiles used in 1-D analyses (indicated as SSECTB1-B2) and showing depths to sample points used for the evaluation of statistical distributions

because it has a low PI=2, which is close to the site average of PI=5. Specimens were prepared with kneading compaction to a range of modified Proctor RC values and water contents, wrapped in a wire-reinforced membrane, and subjected to drained strain-controlled cyclic simple shear testing with vertical strain measurements (ε_v) at a range of cyclic shear strain amplitudes (γ_c). Additional details on the specimen preparation and testing procedures are provided by Wang et al. (2004). Partial results of tests on sample B-3 are synthesized in Fig. 6(a), which shows values of ε_v at 15 cycles of loading $[(\varepsilon_v)_{N=15}]$, corresponding to various RC and as-compacted degrees of saturation (S). The data show that RC is the principal construction-related factor that affects

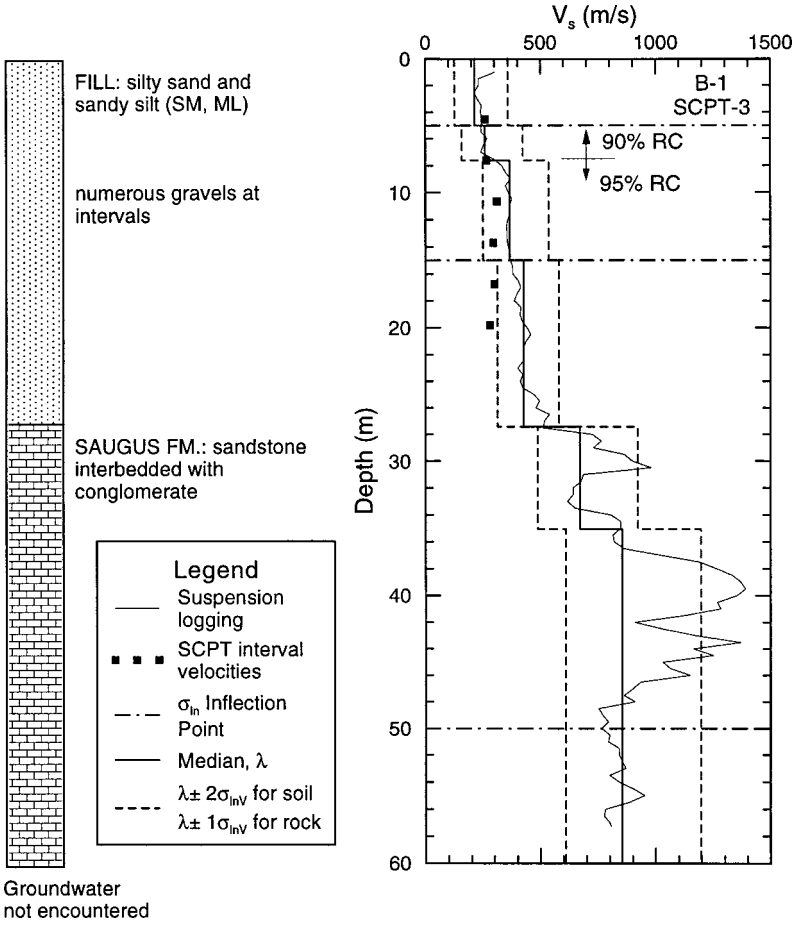

Fig. 4. Representative soil profile at school site near boring location, showing measured shear wave velocity data and range of assumed velocity profiles for analysis

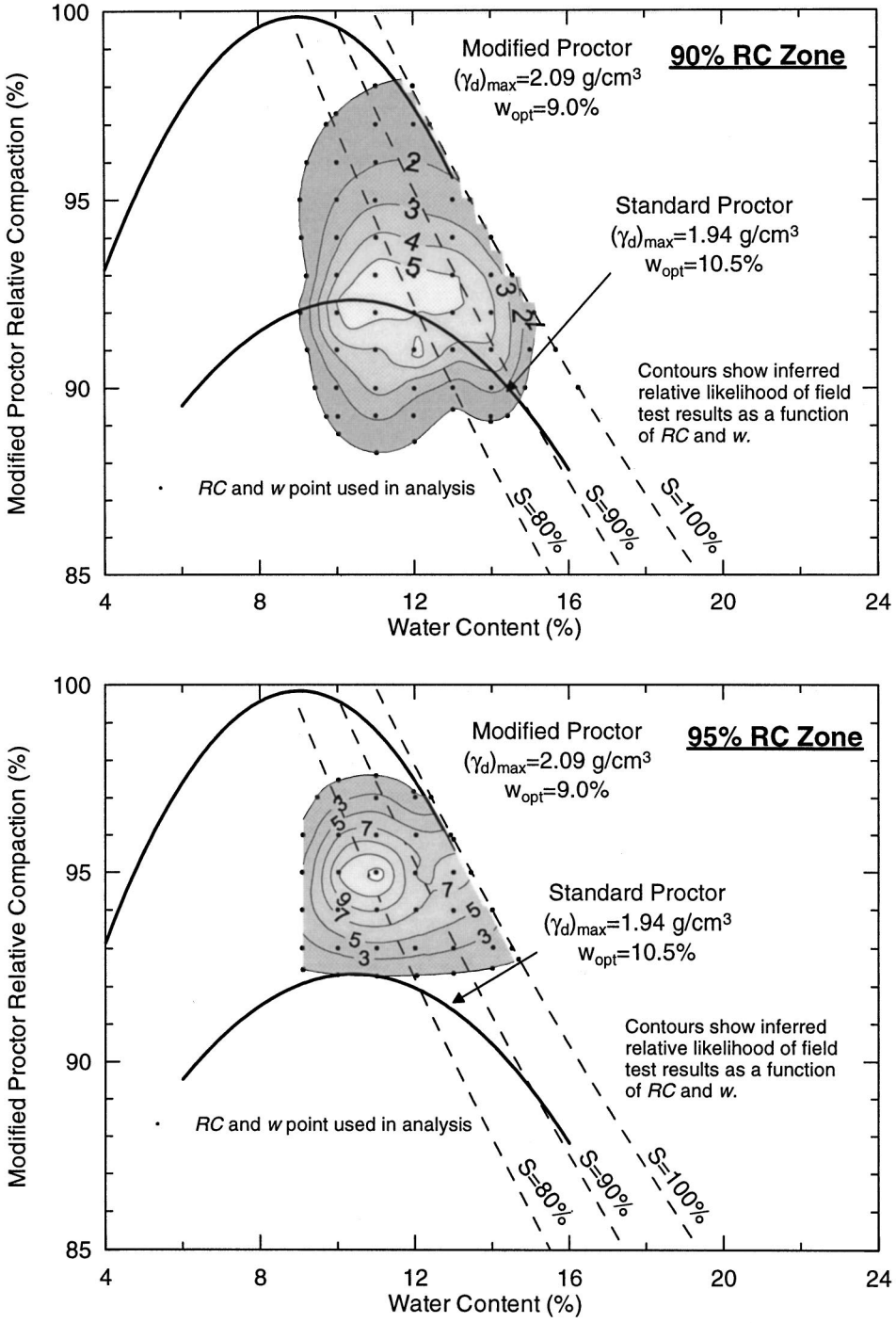

Fig. 5. School site: Compaction curves by standard and modified Proctor standards, contours showing the relative likelihood of compaction conditions based on adjusted field test results from the time of construction, and points used to represent compaction space for estimation of seismic compression

seismic compression (i.e., S is not important). The lack of sensitivity of ε_v to S is attributed to what appears to be consistent macrostructures of soils compacted at high S (wet of the line of optima) and low S (dry of the line of optima) for this low plasticity soil. The variation of vertical strain with the number of strain cycles $[\varepsilon_v/(\varepsilon_v)_{N=15}]$ is shown for sample B-3 in Fig. 6(b) along with the range of $\varepsilon_v/(\varepsilon_v)_{N=15}$ for crystal silica sand (shown for reference only). The curves of $\varepsilon_v/(\varepsilon_v)_{N=15}$ for sample B-3 were found to be insensitive to RC, S and γ_c.

Horizontal and vertical surface displacements at the site are known from pre- and post-Northridge earthquake surveys. The surveys were performed on January 14, 1994 and January 21, 1994 by the same surveyor (the earthquake was on January 17, 1994), and occurred before construction of buildings and other improvements. Horizontal displacements were negligibly small. The settlement data at six monuments on the fill are shown in Fig. 2. The maximum observed settlement was 6.1 cm at monument 3, which is located over about 5.2 m of 90% RC fill and 23.5 m of 95% RC fill. Other monuments generally were underlain by about

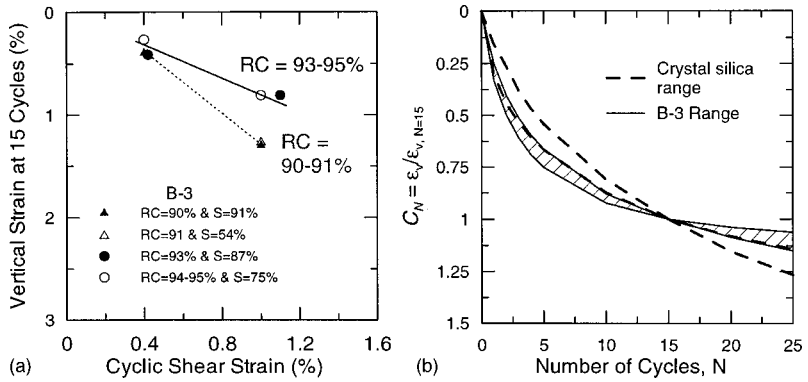

Fig. 6. (a) Seismic compression of soil B-3 from school site; (b) variation of normalized vertical strain with number of cycles for soil B-3 from school site

3.0 m of 90% RC fill and variable depths of 95% RC fill, and experienced 1.3–3.0 cm of settlement.

Site A

As shown in Fig. 1, site A is located about 5 km northwest of the school site and approximately 12.2 km from the 1994 Northridge earthquake fault rupture plane. A plan view and cross section of the approximately 121,400 m^2 site are shown in Figs. 7 and 8, respectively. Preconstruction topography at the site consisted of several deeply incised canyons, with a general increase of elevation to the north. Construction of the fill occurred between July 1990 and August 1991, and involved cuts into the hillside at the north and west ends of the site, and large fills extending to depths of up to 24 m at the south and west ends of the site.

A number of borings were drilled through the fill into rock by Geo/Resources Consultants (San Francisco) and by the writers. Our borings were cased for downhole velocity logging. SCPTs were also performed in the fill. As illustrated by the boring log in Fig. 9, the fill soils consist of silty sandy clay and clayey silty sand and occasional fragments of rocks. Fines contents in the fill range from 43 to 69% (average=53%) and results of Atterberg limit tests are plotted near and slightly above the ''A'' line (average LL=32 and PI=13), generally providing CL or SC classifications by the Unified Soil Classification System. At the base of canyons, the fills are underlain by up to 12 m of sandy, silty clay alluvium. Index test results for the alluvium are similar to those for the fill. Underlying the alluvium and fill soils is bedrock consisting of severely weathered, silty, sandy claystone belonging to the Saugus Formation. Measured interval shear wave velocities from the downhole logging are shown in Fig. 9 along with the site velocity model adopted for use in analysis. Groundwater was not encountered in any of the borings or SCPTs at the site.

Fill placed at the site was required to have a minimum relative compaction of 90% according to the modified Proctor standard. Water content was not controlled during construction, and cut areas were not overexcavated. We reviewed field logs of 1,711 tests that documented water content (w) and dry density (γ_d) at the time of construction. Values of as-compacted modified Proctor relative compaction were evaluated using a consistent set of compaction curves developed in this study from nine bulk samples retrieved at multiple locations across the site. Fig. 10 shows the resulting contours of the relative likelihood of field tests having different values of RC and w. The contour ordinates were developed by discretizing the RC space into 1% intervals and the w space into 1% intervals, calculating the percentage of all tests within each of those bins, and then contouring the resulting data using the Kriging geostatistical gridding method (Cressie 1991). The mode RC is 87.8% and the mode w is 10.5%. Note that the majority of the fill soil appears to have been compacted dry of the line of optima (which occurs at a degree of saturation, $S \approx 82\%$) and at densities below the minimum standard of 90% RC.

Dry density and water content data are also available for the alluvium from tests performed by a project consultant prior to construction. Values of modified Proctor relative compaction computed from these data (using a compaction curve for the alluvium developed in this study) are on the order of 77–85% (average ~80%). Actual RC values should be slightly higher as a result of compression induced by the fill overburden. Based on oedometer tests, the change in volume from fill overburden and minor wetting is estimated to have raised the RC to ~80–87% (average ~83–84%). We recognize the approximation associated with assuming that the alluvium, which is a natural soil, can be adequately characterized by a RC value, which is associated with soil compaction. In particular, compacted laboratory specimens likely have different soil fabric from natural alluvium, and these fabric variations may affect the soil's volume change characteristics. This is discussed further in ''Analysis of Settlements from Seismic Compression.''

Simple shear laboratory testing was performed to evaluate the seismic compression potential of a soil sample from site A (sample A-1) that is representative of the fill and alluvial soil types. This soil is a medium plasticity clay (CL) according to the Unified Soil Classification System, with 54% fines and PI=15. Specimens of samples A-1 were prepared and tested in the same manner described previously for samples B-1–B-3. Partial results of the tests are synthesized in Fig. 11(a), which shows shaded bands of ε_v at 15 cycles of loading $[(\varepsilon_v)_{N=15}]$ corresponding to various RC. The results clearly show significant sensitivity of $(\varepsilon_v)_{N=15}$ to RC. In addition, the results show for intermediate RC (88 and 92%) strong increases of $(\varepsilon_v)_{N=15}$ with a decrease in the as-compacted degree of saturation, S, which is attributed to variations of the macrosoil structure with the compaction condition (clod structure dry of the line of optima; the structure becomes relatively continuous wet of the line of optima) for this soil with plastic fines. At RC=84%, the low compaction energy does not break down clods even at high S, and there is little sensitivity of $(\varepsilon_v)_{N=15}$ to S. The range of $\varepsilon_v/(\varepsilon_v)_{N=15}$ for sample A-1 is shown in Fig. 11(b) along with the range for crystal silica sand (shown for reference only). Parameter $\varepsilon_v/(\varepsilon_v)_{N=15}$ was found to be mod-

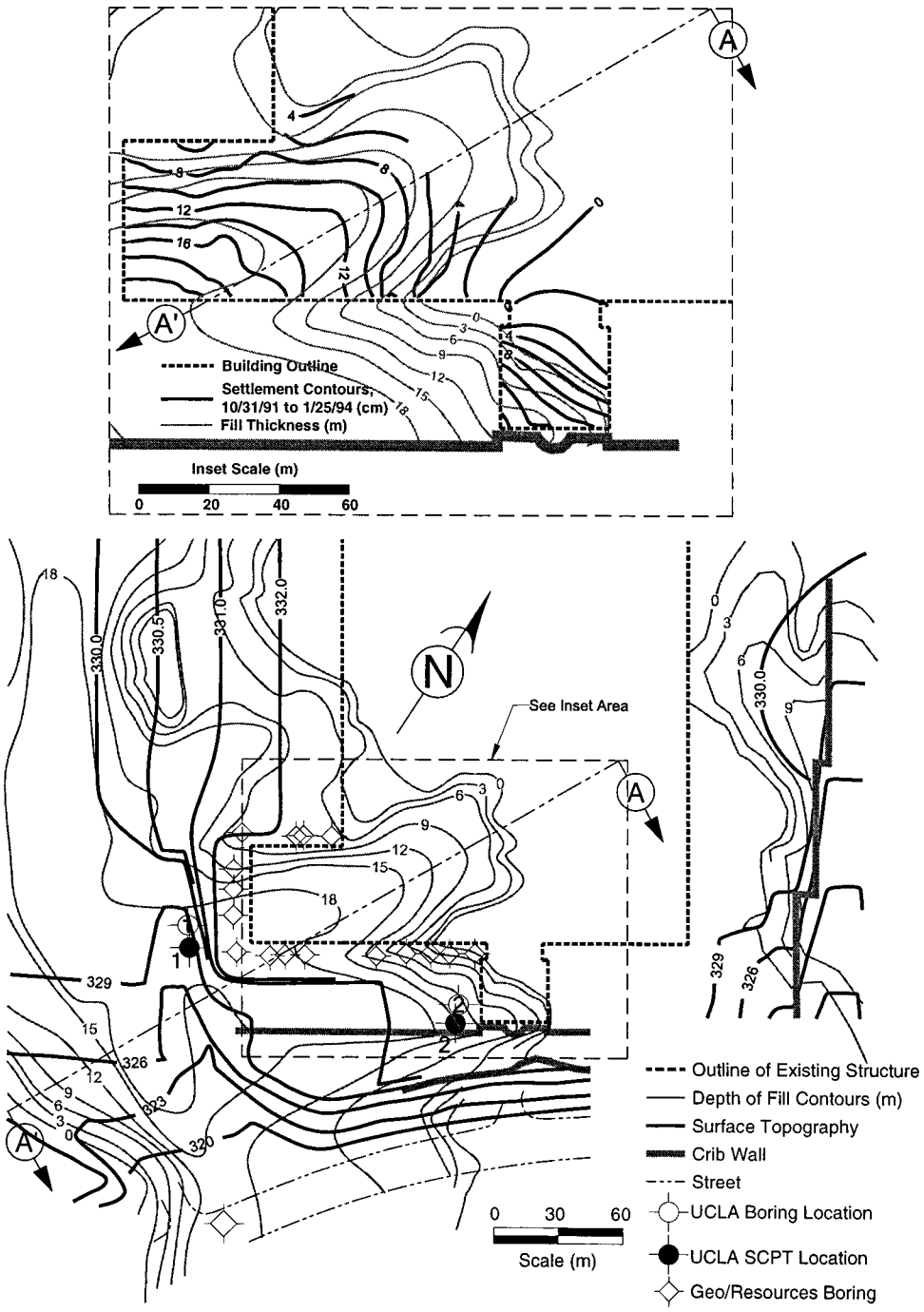

Fig. 7. Plan view of site A, showing fill thickness contours and locations of subsurface exploration; contours of building pad settlement are shown in the inset

erately sensitive to RC, but insensitive to other parameters such as S or γ_c.

Vertical surface displacements at site A were established from pre- and post-Northridge earthquake surveys of floor elevations in the building. Horizontal movement data are unavailable, but significant horizontal deformation was not evident from floor crack patterns or from cracking of pavements outside of the building. The pre-earthquake data are from as-built drawings dated October 31, 1991. Elevations on these drawings were based on a postconstruction survey by a licensed land surveyor and they reflect elevations after the installation of flooring. Postearthquake data are based on a survey (by the same licensed land surveyor) performed on January 25, 1994. Interviews of the surveyor by the writers indicated no change in flooring material, suggesting that the difference in elevation from these two surveys can be used to estimate floor settlements between the specified dates. As shown in the inset of Fig. 7, the maximum observed settlement was 21.6 cm at the southwest corner of the building, which is located over about 20.3 m of fill. The amount of settlement generally increases with the depth of the fill, and no appreciable settlement was measured in cut areas.

Since approximately 26 months elapsed between the pre- and postearthquake surveys, it is likely that some of the observed settlements occurred before the earthquake as a result of hydro-

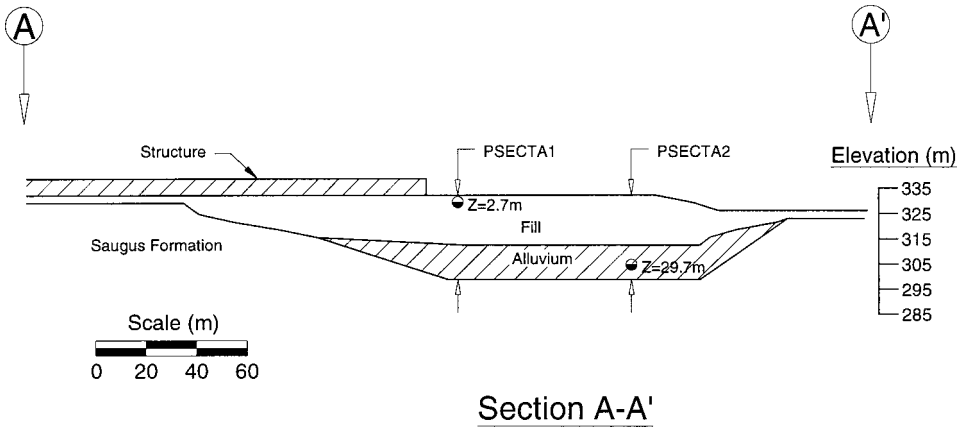

Fig. 8. Cross section A–A′ at site A showing locations of vertical profiles used in 1-D analyses (indicated by PSECTA1-A2) and showing depth to sample points used for evaluation of statistical distributions

compression. Interviews of permanent staff working at site A indicated no perceptible distress from settlement before the earthquake. The staff report noticing significant settlements only after the earthquake and, since they have no financial interest in the cause of the settlement (i.e., they are not participants in legal actions), their statements are considered unbiased. These observations suggest pre-earthquake settlements were small.

Water content data in fill from a 1991 investigation by a project consultant and from our borings in 1998 provide evidence of wetting across the upper ~10 m of the site, with near-surface water contents rising from ~10 to ~14%, which corresponds to a change in degree of saturation from $S \sim 60$ to ~80%. The data suggest that wetting did not occur at depths >15 m. Based on the results of response to wetting tests performed on the fill soils, hydrocompression analyses for a partial wetting condition were performed (using the procedure of Houston 1992) to estimate settlements associated with the above change in saturation. The results suggest that settlements between the dates for which water

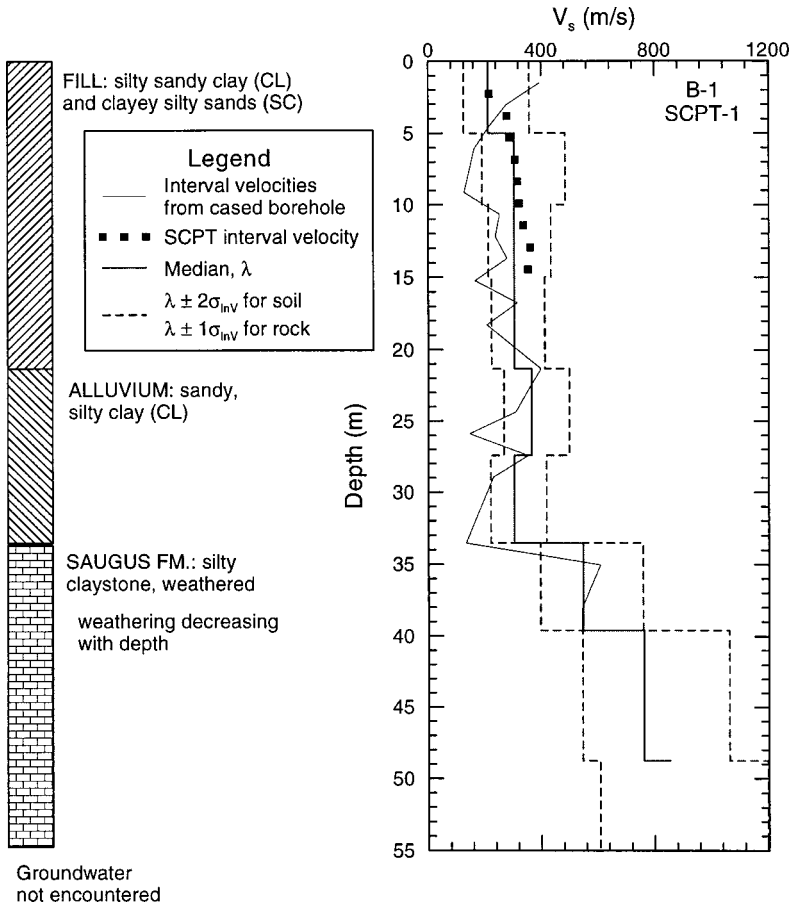

Fig. 9. Representative soil profile site A near boring 1 showing measured shear wave velocity data and range of assumed velocity profiles for analysis

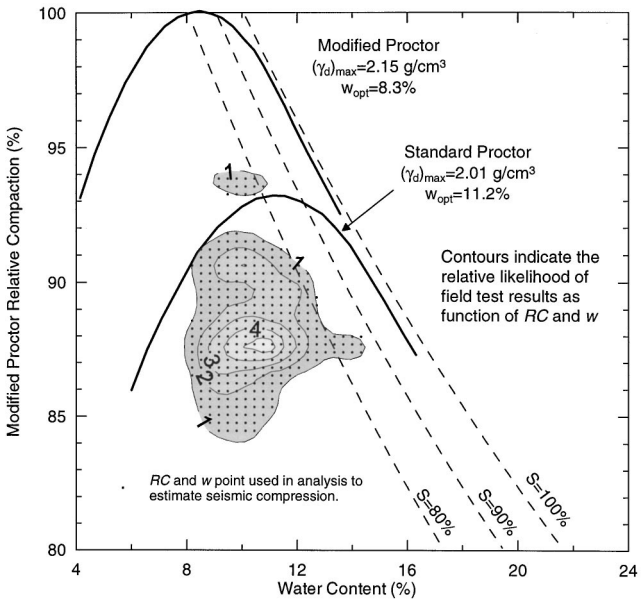

Fig. 10. Site A: Compaction curves by standard and modified Proctor standards, contours showing relative likelihood of compaction conditions based on field tests at the time of construction, and points used to represent compaction space for estimation of seismic compression

contents are available (1991–1998) were likely in the range of 6–20 cm, with a best estimate of 12 cm. Variability in the estimated settlements is associated with variability in the laboratory response to wetting tests.

Because these hydrocompression settlement estimates are based on water content changes between October 1991 and March 1998, we can only speculate as to how much of the hydrocompression settlement occurred by January 1994 (at the time of the earthquake). Natural precipitation between 1991 and 1998 at the nearest weather stations averaged 40 cm/year, which is much less than the water likely introduced into the fill from irrigation of lawns near the building. Because lawn irrigation introduces a consistent rate of infiltration, it would seem reasonable that the fraction of 1998 settlement that had occurred by 1994 would approximately match the ratio of time elapsed since 1991 (this ratio is about 1/3). By this reasoning, the best estimate of 1994 settlement is approximately 4 cm for portions of the site with ⩾10 m of fill, and the likely range of settlements for this fill depth is estimated to be 2–10 cm (allowing for uncertainty in the 1991–1994/1991–1998 settlement ratio).

Estimation of Ground Motions

The objective of ground motion estimation for the school site and site A is to develop a suite of time histories that represent possible realizations of ground shaking on rock beneath the sites during the 1994 Northridge earthquake. Three sources of time histories were used: (1) recordings on rock near the sites; (2) deconvolved ''rock'' motion calculated from recordings at nearby soil sites; and (3) time histories developed from seismological simulations.

The locations of the fill sites relative to the Northridge fault rupture plane and local strong motion stations are shown in Fig. 1. We selected time histories recorded at accelerometers that are close to the fill sites, have similar source-site azimuths to those of the fill sites, and which are not subject to unusual local site effects such as pronounced topographic amplification. The selected accelerometer sites are listed in Table 1 and plotted in Fig. 1. Data for each of these sites were obtained from the Pacific Earthquake Engineering Research Center (PEER) strong motion library (www.peer.berkeley.edu).

Two of the strong motion stations listed in Table 1 [Lake Piru Dam (LPD) and The Jensen Generator Building (GEN)] are located on weathered Saugus rock similar to that underlying the fill sites. The other stations Newhall Fire Station (NFS), Potero Canyon (PC), Castaic Dam downstream (CDD)] are located on shallow soil overlying Saugus bedrock, and deconvolution analyses were performed to estimate the motion on rock from the soil recordings. These calculations were performed according to the procedure of Silva (1986), which follows:

1. Soil recordings are low pass filtered with corner frequency of 15 Hz;
2. Strain-dependent soil properties are evaluated based on 87% of the accelerogram's amplitude using equivalent linear ground response analyses (*SHAKE91*, Idriss and Sun 1991); and
3. Rock motion is calculated for an outcropping condition using strain-dependent soil properties from (2) and the full amplitude of the ground surface accelerogram.

Details on the dynamic soil properties used in these deconvolution analyses were presented by Stewart et al. (2002), along with the recorded and computed wave forms. The deconvolution pro-

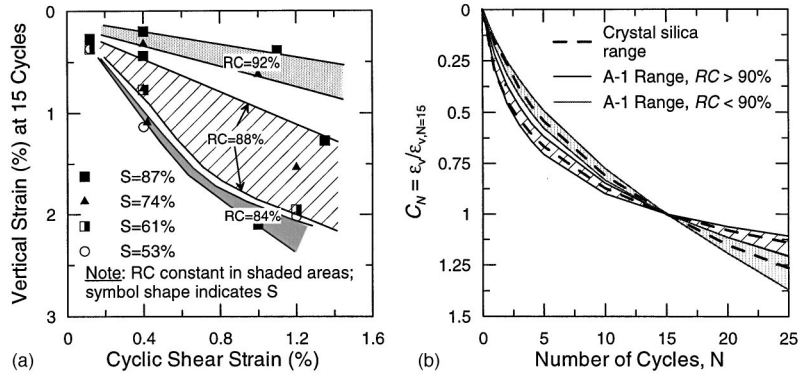

Fig. 11. (a) Effect of RC and *S* on the seismic compression of soil A-1 from site A; (b) variation of normalized vertical strain with the number of cycles and RC for soil A-1 from site A

Table 1. Strong Motion Stations near Subject Fill Sites that Recorded the 1994 Northridge Earthquake and Scale Factors (SFs) Used to Scale Recorded Motion to Provide Estimates of the Ground Motion Amplitude at the School Site and Site A

Station	Instrument owner[a]	Number	Classification[b]	r (km)[c]	Scale factor	
					School	A
Lake Piru Dam (LPD)	CSMIP	285	B/C1	20.2	2.48	1.62
Newhall Fire Station (NFS)	CSMIP	24279	C2	7.1	0.99	0.65
Potrero Canyon (PC)	USC	90056	C2	7.1	0.99	0.65
Jensen Generator Bldg. (GEN)	USGS	655	B	6.2	0.74	0.48
Castaic Dam downstream (CDD)	CDWR	—	C2	18.2	2.24	1.46

[a]CSMIP=California Strong Motion Instrumentation Program; USC=Univ. of Southern California; USGS=U.S. Geological Survey; and CDWR =California Department of Water Resources.
[b]Classification scheme from Rodriquez-Marek et al. (2001): B=intact rock; C1=weathered soft rock; and C2=shallow soil over rock.
[c]r=closest distance to Northridge fault rupture plane by Wald and Heaton (1994).

cess did not significantly affect the phase and frequency content of the time histories, and values of peak horizontal acceleration generally changed $<30\%$.

In addition to the recorded ground motions, additional synthetic time histories were generated for the fill sites by Dr. Walter Silva using a stochastic finite source model of the Northridge earthquake. General features of this method of simulation are described by Silva et al. (1990). The resulting time histories were presented by Stewart et al. (2002).

As indicated in Table 1, the strong motion stations near the fill sites have different site-source distances (r) than those at the school site or site A (for which $r=7.2$ and 12.2 km, respectively). Accordingly, the recorded (and recorded-deconvolved) time histories were scaled to provide estimates of the time histories at the fill sites. We scaled the time histories using a scaling factor (SF) that is based on distance scaling from an empirical attenuation relationship [Abrahamson and Silva (AS) 1997],

$$\mathrm{SF}=\frac{\mathrm{avg}[S_{a,\mathrm{site}}(T=0:0.3s)]}{\mathrm{avg}[S_{a,\mathrm{SMA}}(T=0:0.3s)]} \tag{1}$$

where $S_{a,\mathrm{site}}$ and $S_{a,\mathrm{SMA}}$ denotes the AS median predictions for the fill and strong motion accelerometer (SMA) sites, respectively, and $T=0:0.3s$ indicates that average spectral accelerations over the indicated period range were used (because distance scaling in the AS relationship is period dependent). The use of the short period range for scaling was motivated by the relatively large sensitivity of the computed shear strain to peak acceleration. The resulting scale factors are listed in Table 1.

Various ground motion intensity measures calculated from the prescaled and scaled time histories are presented in Table 2. Due to the promixity of the sites to the fault, the time histories are rotated into the fault strike-normal (fn) and fault-parallel directions (fp). Parameters PHA, PHV, and PHD in Table 2 indicate peak horizontal acceleration, peak horizontal velocity, and peak horizontal displacement, respectively.

Analysis of Settlements from Seismic Compression

Overview of Analysis Approach

The general objectives of backanalyses of the fill sites are (1) to identify whether seismic compression analyses can explain the observed ground displacements and (2) to evaluate the sensitivity of calculated settlements to the variability in input parameters as well as the dispersion of calculated settlements given the overall parametric variability. The seismic compression analyses were performed using the following procedure.

1. The site stratigraphy is evaluated, especially the distribution of fill depth across the site. In situ measurements of shear wave velocity in the fill and underlying native materials are made. Results of this step of analysis are presented in Figs. 2–4 and 7–9.
2. The fill compaction conditions are characterized, including their mean and the distribution about the mean (Figs. 5 and 10).
3. Earthquake ground motion time histories are selected that are appropriate for the site condition present beneath the fill. In forward analyses, the records should be scaled to the PHA obtained from appropriate ground motion hazard analyses, although in the backanalyses employed here, nearby recordings are scaled in the manner described in ''Estimation of Ground Motion.'' A suite of scaled time histories is needed to characterize the natural variability of phase and frequency content of motion that might occur during the design event. At a minimum, 5–10 time histories should be considered in the analyses.
4. Ground response analyses are performed using the input motions and site models. These calculations are often performed using one-dimensional (1-D) and two-dimensional (2-D) representations of the site geometry and equivalent-linear modeling of dynamic soil behavior (programs *SHAKE91*, Idriss and Sun 1991 and *QUAD4M*, Hudson et al. 1994, respectively). Two-dimensional analyses are desirable for sites with irregular surface topography or irregular subsurface stratigraphy. The distribution of peak shear strain (γ_{pk}) in the fill mass is assessed from the ground response analysis results. In addition, the number of shear strain cycles (N) is assessed using procedures outlined by Liu et al. (2001) and Stewart et al. (2002).
5. Volumetric strain (ε_v) is evaluated from shear strain using an appropriate volumetric strain material model. This involves estimating ε_v at 15 cycles of shaking $[(\varepsilon_v)_{N=15}]$ based on the effective shear strain ($\gamma_{\mathrm{eff}}=0.65\gamma_{pk}$), adjusting $(\varepsilon_v)_{N=15}$ for the actual number of cycles (N) using an appropriate $\varepsilon_v/(\varepsilon_v)_{N=15}$ value, and multiplying the result by 2 to account for multidirectional shaking effects (Pyke et al. 1975). For clean sand, the volumetric strain models presented by Silver and Seed (1971) can be used for these analyses. For the soils at the two subject sites, which contain significant fines, site-specific test results are used (Figs. 6 and 11).

Table 2. Characteristics of Input Time Histories for Response Analyses

Recording	Duration (s)[a]	N[b]	T_m (s)[c]	As recorded				Scaled for school site				Scaled for site A			
				PHA (g)	PHV (cm/s)	PHD (cm)	$I_{a,\max}$ (cm/s)[d]	PHA (g)	PHV (cm/s)	PHD (cm)	$I_{a,\max}$ (cm/s)	PHA (g)	PHV (cm/s)	PHD (cm)	$I_{a,\max}$ (cm/s)
CDD (fn)	5.3	18.1	0.74	0.19	31.1	13.9	64.3	0.43	69.6	31.0	322.9	0.28	45.4	20.2	137.2
CDD (fp)	3.6		0.59	0.27	21.5	7.2	60.9	0.61	48.2	16.2	305.8	0.40	31.4	10.6	129.9
LPD (fn)	5.3	16.3	0.57	0.27	26.6	10.2	62.3	0.66	65.9	25.3	383.4	0.43	43.0	16.5	163.6
LPD (fp)	6.7		0.61	0.22	25.1	8.6	44.0	0.55	62.1	21.3	270.5	0.36	40.6	13.9	115.4
NFS (fn)	3.2	19.9	0.60	0.61	83.8	33.4	429.8	0.61	83.0	33.0	421.2	0.40	54.5	21.7	181.6
NFS (fp)	2.9		0.37	0.59	38.7	15.0	344.5	0.58	38.3	14.8	337.7	0.38	25.1	9.7	145.6
GEN (fn)	4.2	10.2	0.87	0.51	65.7	47.6	263.1	0.38	48.6	35.2	144.1	0.25	31.8	23.0	61.6
GEN (fp)	3.6		0.53	0.99	66.1	26.5	708.1	0.74	48.9	19.7	388.0	0.48	32.0	12.8	165.9
PC (fn)	1.7	6.1	1.73	0.35	107.1	42.1	128.8	0.34	106.1	41.7	126.4	0.22	69.4	27.3	54.0
PC (fp)	4.0		1.39	0.27	64.8	27.3	70.7	0.27	64.1	27.1	69.3	0.17	41.9	17.7	29.6
PE&A A	3.5	10.8	0.53	—	—	—	—	—	—	—	—	0.29	26.6	17.0	61.3
PE&A School	3.1	14.5	0.58	—	—	—	—	0.41	51.4	29.7	168.7	—	—	—	—

[a]Calculated from a Husid plot as time between 0.05 and 0.75 normalized Arias intensity.
[b]Equivalent number of uniform strain cycles; calculated as vector sum normalization of both horizontal components using a general procedure by Liu et al. (2001) and customized for seismic compression by Stewart et al. (2002).
[c]Mean period derived from Fourier spectral amplitudes defined by Rathje et al. (1998).
[d]Arias intensity of ground motion (Arias 1970).

6. Ground settlements are evaluated by integrating volumetric strain over the height of the section of fill.

For the analyses performed in this study, 2-D ground response analyses were performed along the cross sections shown in Figs. 3 and 8 (additional perpendicular sections were analyzed by Stewart et al. 2002). The finite-element meshes used in these 2-D analyses have large lateral dimensions to minimize boundary effects. Moreover, element heights are smaller than one-tenth of the 10-Hz wavelengths to maintain computational accuracy. Additional 1-D analyses were performed at the locations marked SSECT and PSECT in Figs. 3 and 8.

In addition to seismic compression, ground movement from permanent shear deformation in soil was also considered. However, limit-equilibrium slope stability calculations performed using conservative strength parameters provide yield accelerations that exceed the maximum horizontal equivalent accelerations within reasonable slide mass geometries. Consequently, permanent shear deformation was unlikely to have influenced the observed settlements.

Most of the parameters used in seismic compression/settlement analyses have measurement or estimation uncertainty. We quantify our uncertainty in model parameters, and incorporate these uncertainties into the settlement calculations. This is performed using a logic tree approach that is described in the following.

Estimation of Parameter Values and Weights

Parameters/quantities required to implement the seismic demand and volumetric strain models described in ''Overview of Analysis Approach'' include curves for reduction of the shear modulus and increase of soil hysteretic damping with shear strain amplitude, profiles of shear wave velocity (V_s), ground motion time histories, and the compaction condition of fill soils (RC and *S*). Uncertainties associated with estimation of these parameters/quantities are propagated through the analysis using a logic tree approach, which allows the use of alternative realizations of model parameters, each of which is assigned a weight. The weights for all possible realizations of a parameter sum to unity. Each calculated settlement value corresponds to a unique combination of parameter realizations (i.e., a path through the logic tree), and the weight belonging to that settlement value is the product of all the weights in the path. The sum of the weights for all computed settlement values is unity.

Two models for the modulus reduction and damping behavior of the soil were selected based upon the fill soils' index properties. One of these curve pairs is the upper-bound modulus reduction curve and lower bound damping curve for sand published by Seed and Idriss (1970) (referred to as the ''sand'' curves), while the other curve pair is the PI=15 clay curves by Vucetic and Dobry (1991) (referred to as the ''clay'' curves). These two curve paris are fairly similar, so parametric variability in this case is small. For both sites, equal weights of 0.5 are assigned to each curve pair. Underlying weathered Saugus bedrock materials were modeled with the ''sand'' curves.

The shear wave velocity data from the fill sites were presented in Figs. 4 and 9, in which also are best estimate velocity profiles, which are indicated by solid lines, denoted median, λ in the legend. The dashed velocity profiles denoted in the legend as $\lambda \pm 2\sigma_{\ln V}$ or $\lambda \pm 1\sigma_{\ln V}$ span the expected range of variability as a function of depth, and correspond to the stated number of standard deviations above and below the median based on a log–normal distribution. Variations of $\pm 1\sigma_{\ln V}$ were used in rock,

compared to $\pm 2\sigma_{\ln V}$ in soil, because $>1\sigma_{\ln V}$ variations of rock velocity from the median produced unrealistic V_s values relative to the field measurements. The standard deviation values (i.e., $\sigma_{\ln V}$) used to establish these limits in velocity were taken from an empirical model (Toro 1997).

Using the median V_s profiles, $\sigma_{\ln V}$, and a depth-dependent correlation coefficient for velocity given by Toro (1997), we generated 15 random V_s profiles for each site. Details of the profile generation process and lists of individual profiles were presented by Stewart et al. (2002). The velocity profile realizations are not randomly distributed across the velocity ranges shown in Figs. 4 and 9, but instead tend to be clustered near the median in accordance with the log–normal distribution. Equal weight is assigned to each profile. Constraints were placed on the generation of these profiles by disallowing V_s realizations beyond the $\pm 2\sigma_{\ln V}$ limit for soil and $\pm 1\sigma_{\ln V}$ for rock. These constraints were added to avoid unreasonable realizations of V_s.

Characteristics of the ground motion time histories selected for use with each fill site are in Table 2. Recalling that the recorded time histories had to be scaled for use at the fill sites because of nonequal site-source distances, we estimate the quality of a recording for a fill site by the departure of SF from unity (SF is a valid index of ''quality'' because all selected recordings have site-source azimuths similar to those for the fill sites). Using this concept, the relative likelihood for individual ground motion (L_{gm}) with respect to a fill site is calculated as follows:

$$L_{gm\ i}(\mathrm{SF}_i) = \begin{pmatrix} \mathrm{SF}_i & \text{if } \mathrm{SF}_i \leqslant 1 \\ 1/\mathrm{SF}_i & \text{if } \mathrm{SF}_i > 1 \end{pmatrix} \quad (2)$$

L_{gm} for synthetic time histories is arbitrarily taken to be one-half the value from the least likely recorded time history. Weight factors for individual ground motions are directly proportional to the relative likelihood values; the weights are simply normalized so that they sum to unity.

Compaction conditions for the fill soils were weighted according to the relative likelihood contours described previously. Fig. 5 shows contours that depict the relative likelihood of compaction conditions at the school site in both the 90 and 95% RC zones along with a series of RC and *w* coordinates used to discretize the compaction space for a likelihood greater than 1%. Fig. 10 presents similar information for site A. The logic tree for each site has a branch for each of the compaction coordinates in either Fig. 5 or 10. The effective compaction condition of the alluvium at site A is fixed at RC=84%, which is close to the estimated average, RC≈83–84%. Recall that the volumetric strain for this material at these low RC values is not sensitive to the as-compacted degree of saturation (*S*). As noted previously, an unknown bias may exist in laboratory test results on compacted specimens relative to natural in situ alluvium. It is important to keep this added epistemic uncertainty in mind when interpreting the results of analysis for portions of site A underlain by significant alluvium.

Interpretation of Analysis Results

Peak shear strains within the fill mass (γ_{pk}) are evaluated through the use of 1-D and 2-D ground response analyses. Volumetric strains (ε_v) are then evaluated, and are integrated across the thickness of the fill section to estimate settlement. Parameters γ_{pk} and ε_v are referred to as *response quantities*. A given set of input quantities for analysis of a response quantity is referred to as an *input vector*, which for seismic compression analysis consists of a single time history, a single V_s profile, a single compaction condition (i.e., values of RC and *w*), and a particular pair of modulus reduction and damping curves. Corresponding to each input vector are single realizations of each response quantity to which weights are assigned based on the product of the weights associated with each element of the input vector. Since the weight (or likelihood) of each realization of a response quantity is known, a weighted frequency function (WFF) for the response quantity can be constructed. The WFF, which is analogous to a probability mass function, is constructed by subdividing the numerical domain of the response quantity into bins, and for each bin summing the weights associated with all realizations of the response quantity.

Table 3. Median and Standard Deviation Parameter Estimates of Peak Shear Strain (γ_{pk}) at Selected Locations, School Site and Site A

Site	Analysis type	Location	Depth (m)	Median, λ (%)	Std. dev., $\sigma_{\ln}$
School	2-D	Ssectb1	18.6	0.06	0.50
		Ssectb2	10.5	0.04	0.59
	1-D	Ssectb1	18.6	0.07	0.64
		Ssectb2	10.5	0.10	0.80
A	2-D	Psecta1	2.7	0.07	0.74
		Psecta2	29.7	0.10	0.72
	1-D	Psecta1	2.7	0.04	0.91
		Psecta2	29.7	0.20	0.73

Analysis Results for Maximum Shear Strain

At each of four statistical sample locations shown in Figs. 3 and 8 (e.g., PSECTA1, $z=2.7$ m), shear strain WFFs were evaluated, and were found to be approximately log normally distributed based on chi-square and Kolmogorov–Smirnov (KS) distribution tests (details of statistical testing were presented by Stewart et al. 2002). Accordingly, we represent the distribution of peak shear strain (γ_{pk}) across the fill domain using the median in linear units (λ) and the standard deviation in natural logarithmic units ($\sigma_{\ln}$). Examples of these statistical moments are presented in Table 3 for the statistical sample locations.

Selected profiles of $\lambda \pm 1\sigma_{\ln}$ shear strain calculated by 2-D analyses at the fill sites are shown in the top frames of Figs. 12 and 13 along with 1-D median profiles (λ). The calculated shear strain is generally larger than the typical threshold strain for silty sand (0.01–0.05%; Vucetic 1994), suggesting that nearly the full depth of fill likely contributed to the observed settlement. As expected, shear strains generally increase with depth near the surface of fills, and change sharply at impedance contrasts. The largest shear strain in the profiles most often occurs above impedance contrasts, within the upper 10 m of fill, but in some nearly 1-D profiles it may occur at depth above fill/alluvium or fill/bedrock interfaces.

Overall comparisons of the 1-D and 2-D analysis results in Figs. 12 and 13 and Table 3 reveal three trends: (1) for horizontally layered soils behind a slope face (site A), median shear strain from the 2-D analyses exceed those from 1-D analyses to depths that correspond roughly to the base-of-slope elevation; (2) the presence of a sloping impedance contrast (i.e., bedrock soil, or adjacent fill layers) provides additional lateral restraint to the overlying, softer layer, which reduces 2-D strains relative to 1-D strains (e.g., near the base of fill at both sites); and (3) 2-D strains have smaller dispersion (measured by $\sigma_{\ln}$) than 1-D strains.

The 2-D analysis results were studied to evaluate the sensitivity of peak shear strains to variations in the input ground motion and variation of dynamic soil properties. Sensitivity analyses for a

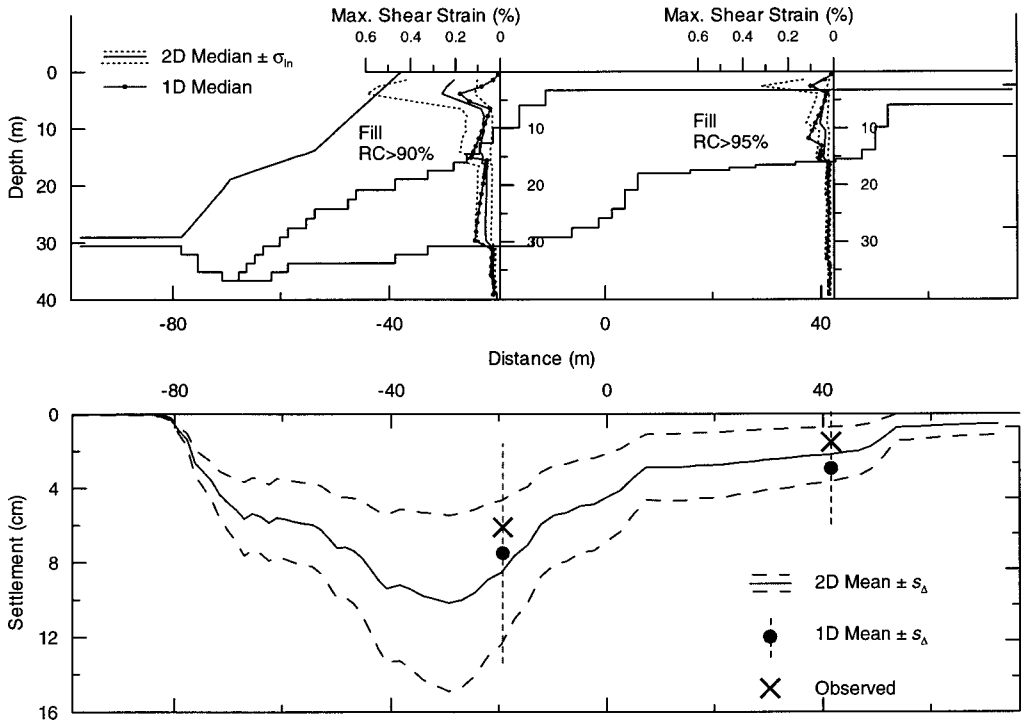

Fig. 12. School site, section B–B′: Vertical profiles of shear strain from 2-D and 1-D analyses (top frame) and lateral profiles of observed and calculated settlement (bottom frame)

particular parameter (say, V_s) involve fixing the parameter at multiple values that span the parameter space, and examining the resulting variation of shear strain median. The reduction of dispersion associated with fixing the parameter is also investigated. As described in detail by Stewart et al. (2002), these sensitivity studies reveal that median shear strain is strongly influenced by shear wave velocity and ground motion characteristics, but is not significantly influenced by the choice of modulus reduction/damping curves in this particular case.

Median shear strains decrease with an increase of average V_s in fill, which is expected. Among the ground motion intensity measures considered, strains were found to increase significantly

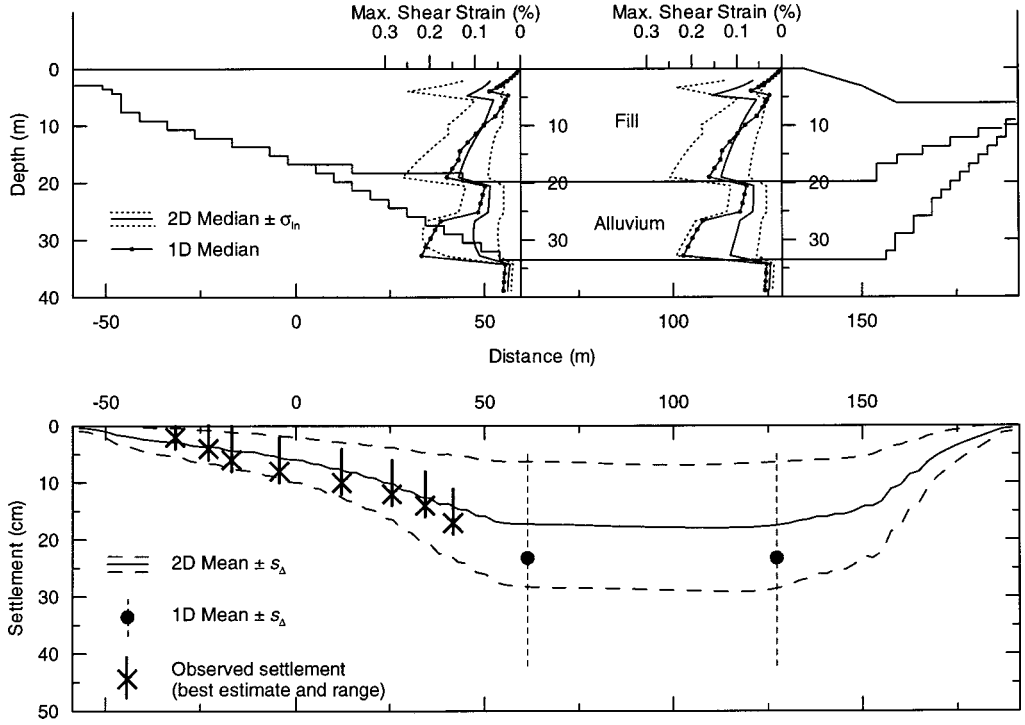

Fig. 13. Site A, section A–A′: Vertical profiles of shear strain from 2-D and 1-D analyses (top frame) and lateral profiles of observed and calculated settlement (bottom frame)

Table 4. Point Estimates of Volumetric Strain (ε_v) at Selected Locations, School Site and Site A

Site	Analysis type	Location	Depth (m)	Weighted Avg (%)	Std dev (%)	Coefficient of variation
School	2-D	SSECTB1	18.6	0.18	0.10	0.54
		SSECTB2	10.5	0.10	0.09	0.92
	1-D	SSECTB1	18.6	0.21	0.13	0.60
		SSECTB2	10.5	0.24	0.17	0.68
A	2-D	PSECTA1	2.7	0.34	0.32	0.94
		PSECTA2	29.7	0.84	0.73	0.86
	1-D	PSECTA1	2.7	0.18	0.26	1.42
		PSECTA2	29.7	1.50	1.12	0.74

with an increase of PHA, but to be relatively insensitive to PHV. The shear strains are also affected by resonance effects between the input motion and site, with the largest shear strains occurring when the mean period (T_m) of ground motion is similar to the site period. Standard deviation of the shear strain is most strongly influenced by variations in V_s and by input ground motion.

Analysis Results for Volumetric Strain

At each of the statistical sample locations used for shear strain, volumetric strain WFFs were calculated and compared to numerous forms of probability density functions (normal, log–normal, shifted log–normal, and extreme value distributions). As discussed in detail by Stewart et al. (2002), none of these theoretical models matches the WFFs well, although the normal distribution is among the most effective based on the chi-square test. We represent the distribution of the volumetric strain (ε_v) response quantity by the weighted mean ($m_{\varepsilon v}$) and weighted standard deviation ($s_{\varepsilon v}$). These quantities happen to correspond to statistical moments of a theoretical normal distribution, although it should be emphasized that the data are not normal. The $m_{\varepsilon v}$ and $s_{\varepsilon v}$ values are presented in Table 4.

As with shear strain distributions, volumetric strains generally increase with depth from the surface of the fills, and change sharply at impedance contrasts. The largest volumetric strains generally occur at shallow impedance contrasts or at the base of fill. Sensitivity analyses similar to those described previously indicate that calculated median volumetric strain is most sensitive to the compaction condition and to the shear strain amplitude. Volumetric strain increases as compaction conditions become less favorable, which generally occurs with a decrease in as-compacted water content and decrease in relative compaction. Volumetric strain is very strongly dependent on the shear strain amplitude, and thus is dependent on those factors that control the shear strain amplitude (V_s, PHA, and to a lesser extent, T_m). The dependence of volumetric strain on the equivalent number of uniform strain cycles (N) was second-order relative to the above dependences on shear strain and the compaction condition. The primary factor that controls the coefficient of variation of volumetric strain is variability in shear strain, which in turn is principally controlled by variability of the V_s profiles and the input ground motion.

Comparison of Predicted and Observed Settlements

Shown in the bottom frames of Figs. 12 and 13 are the observed field settlements along the sections at the two fill sites along with settlements calculated from 2-D and 1-D analyses (the field settlement ranges shown in Fig. 13 by the vertical lines are associated with the uncertainty in estimated pre-earthquake hydrocompression settlements). The calculated settlement quantities are presented as weighted mean (m_Δ) and mean$\pm$one standard deviation ($m_\Delta \pm s_\Delta$) values in arithmetical units. This was done to mimic the above presentation of results for volumetric strain, which is related to settlement through simple integration over the soil depth. Settlement predictions derived from the 2-D ground response analyses are represented by continuous curves. The 1-D analysis predictions are shown by discrete symbols at appropriate locations along the sections. Observed and calculated settlements are tabulated in Table 5 for the SSECT and PSECT statistical sample locations (shown in Figs. 3 and 8).

For the school site (Fig. 12), settlement predictions from 2-D analyses generally compare favorably to observed field settlements. For the site as a whole (including sections analyzed by Stewart et al. 2002 but not presented here), the observed settlements are between the 30th and 70th percentile predictions, and the comparisons are generally suggestive of no systematic bias in model predictions.

For site A (Fig. 13), the mean settlement predictions from the 2-D analyses generally slightly underpredict ''best estimate'' field settlements, although the trend of the calculated settlements along the section is consistent with observation. The best estimate field settlements are generally consistent with about the 50th–70th percentile of calculated settlements. There are several plausible explanations for this apparent bias in the mean.

1. The location and depth of alluvium along the left (north) side of the section is not known well (drilling to identify the alluvial depth in this area was not possible because it is overlain by a structure). The location of the edge of alluvium shown in Figs. 8 and 13 is assumed based on top-of-alluvium elevations from boreholes south of the building. However, because the section passes up through a natural canyon (see Fig. 7), it is possible that alluvium extends further up the canyon, and that this alluvium contributed additional seismic compression not accounted for in our analyses.
2. The volumetric-shear strain relationship used for the fill soil may contain bias related to larger clods in the field than in

Table 5. Calculated and Observed Field Settlements, School Site and Site A

	1-D analyses			2-D analyses			
	Weighted average (cm)	Standard deviation (cm)	Coefficient of variation	Weighted average (cm)	Standard deviation (cm)	Coefficient of variation	Observed settlement (cm)
School SSECTB1	7.5	5.9	0.78	8.5	3.9	0.45	6.1
School SSECTB2	2.9	3.0	1.02	2.2	1.5	0.67	1.5
Site A PSECTA1	23.2	18.9	0.81	17.3	11.0	0.64	16–21[a]
Site A PSECTA2	23.2	18.9	0.81	17.4	11.0	0.64	*

Note: $*$=settlement for this section could not be reasonably estimated.
[a]Settlement at this location estimated based on nearby measurements (at edge of building).

the laboratory-prepared specimens. The tendency of the site A soils to form clods was documented by Whang et al. (2004). Laboratory specimens with controlled clod size were prepared by sieving. Larger clods could be present in the field, which would lead to a larger interclod void space and thus potentially greater seismic compression susceptibility.

3. The best estimate field settlements could be overpredicted if the pre-earthquake hydrocompression settlements were under-predicted.

Similar results for another cross section at site A were presented by Stewart et al. (2002). The contribution of alluvium to the calculated settlements along section A–A at site A ranges from null (where alluvium is absent) to about 50% (between distance stations 50 and 150 m). Due to the significant contribution of alluvium to the settlements in this portion of the site, and the uncertainty regarding the soil fabric effects on volumetric strain in alluvium (which may introduce unknown bias in our analysis results), we have less confidence in calculated settlements for those portions of the site underlain by significant thicknesses of alluvium.

As shown in Fig. 13, for site A, the calculated settlements derived from 1-D and 2-D analyses differ significantly. The 1-D settlements are larger because the 1-D calculations do not restrain shear strain at depth, which occurs in the 2-D analyses as a result of the bowl-shaped bedrock–soil interface. For the school site (Fig. 12), the 1-D and 2-D settlements are similar as a result of compensating differences, i.e., 2-D volumetric strains exceed 1-D near the surface of the fills, while 1-D strains exceed 2-D near the base. As shown in Table 5, coefficients of variation (COV) for the settlements from 2-D analyses range from about 0.5 to 0.7. Larger settlement COVs of 0.8–1.0 are obtained from the 1-D analyses.

Site-specific analyses of the type presented above are beyond current standards of practice. The prevailing seismic compression analysis procedure used at present is the Tokimatsu and Seed (TS) (1987) simplified procedure, which has several shortcomings for application to the present sites. First, the TS volumetric strain material models are based on simple shear test results for clean sand, which cannot account for the effects of fines content and fines plasticity. Second, the TS procedure evaluates the variation of shear strain amplitude with depth using a stress reduction factor developed for 1-D conditions. As noted previously, this can introduce bias for sites with 2-D geometries.

To illustrate the shortcomings of the T&S analysis procedure for the subject sites, the procedure is applied using average energy- and overburden-corrected standard penetration test (SPT) blow counts of $(N_1)_{60}=28$ and 34 blows/ft, respectively, in the 90 and 95% RC fill at the school site and $(N_1)_{60}=25$ and 10 blows/ft, respectively, in the fill and alluvium at site A. Shear wave velocities for these analyses were taken from site-specific in situ testing, and the PHAs used in the calculations are the mean values from ground response analyses at the sites ($\sim 0.88g$ at the school site, $\sim 0.60g$ at site A; Stewart et al. 2002). The outcome of these calculations is estimated settlements that are approximately twice those shown in Table 5 for the case of 1-D analysis. This overestimation is not surprising because of the aforementioned shortcomings of the TS procedure for these sites.

Conclusions

The objectives of the work described in this paper were to document two case histories of seismic compression, to identify whether a rational analysis of seismic compression for these sites could explain the observed settlements, and to evaluate the sensitivity of calculated settlements to variability in input parameters as well as dispersion of calculated settlements given the overall parametric variability.

The analytical studies of seismic compression indicate that at the school site observed settlements are matched by calculated ground settlements from seismic compression between the 30th and 70th percentile levels. At site A the observed settlements are themselves uncertain, but best estimate settlements are slightly underpredicted by the mean analysis results (i.e., the 50th–70th percentile of calculated settlements match observed field settlements). We speculate that the apparent underprediction at site A results from imperfect knowledge of the site stratigraphy, underestimation of volumetric strain from the laboratory tests as a result of the nonreproducibility of the field soil's large clod structure, and/or uncertainty in the estimated earthquake-induced settlements. While the comparisons to data from these two sites are inadequate from a statistical perspective to conclusively demonstrate the presence of bias or lack of bias in the analysis procedure, these comparisons do provide confidence that site-specific analysis can provide reasonable estimates of the general magnitude of seismic compression-induced ground displacements. Moreover, the results presented herein suggest that a site-specific analysis of the type presented here provides a more effective means by which to estimate ground settlements from seismic compression than the existing Tokimatsu and Seed (1987) procedure.

The mean value of calculated settlements is highly sensitive to the shear strain amplitude and compaction condition, whereas the standard deviation is strongly influenced by variability in the shear strain. The median and standard deviations of shear strain, in turn, are strongly influenced by the site shear wave velocity profile, ground motion characteristics, and method of site response analysis (i.e., 1-D versus 2-D). The various sources of parametric variability combine to form a coefficient of variation for settlements of about 0.5–1.0, closer to the low end of the range if 2-D analyses are performed ($\sim$0.5–0.7) and the upper end of the range if 1-D analyses are performed ($\sim$0.8–1.0).

Several caveats should be noted with respect to use of the procedures employed herein. First, these analyses do not provide an estimate of lateral ground displacement that may arise from seismic compression of soil sections with significant static shear stress. This can be accounted for by integrating volumetric strain in the direction of the major principal stress in lieu of the more common practice of integrating vertically across the fill thickness. Second, engineers should also consider the potential for permanent shear deformation, especially when significant driving static shear stress and weak slope materials are present.

Acknowledgments

The writers would like to thank the following for support of this work: U.S. Geological Survey, National Earthquake Hazards Reduction Program, Award No. 1434-HG-98-GR-00037; a CAREER grant from the National Science Foundation (NSF) (Award No. 9733113); the Pacific Earthquake Engineering Research Center's Program of Applied Earthquake Engineering Research of Lifeline Systems with funding from the Pacific Gas and Electric Company (PEER) (Award No. Z-19-2-133-96); and the University of California, Los Angeles, (UCLA) Department of Civil and Environmental Engineering. This work made use of Earthquake Engineering Research Centers Shared Facilities supported by the National Science Foundation under Award No.

EEC-9701568. The views and conclusions contained in this document are those of the writers and should not be interpreted as necessarily representing official policies, either expressed or implied, of the U.S. government. The writers would like to thank the following individuals who provided materials that were of assistance in this research program: Del Yoakum of Geosoils, Jim Roberts of Jacobs Engineering, and Mike Sisson and Jerod Cascadden. They acknowledge technical assistance for the laboratory testing program provided by Michael Riemer of UC Berkeley. Supportive work by Professor Daniel Pradel at UCLA and of UCLA undergraduate and graduate students Trolis Niebla, Mathew Moyneur, and Annie Kwok is also acknowledged.

References

Abrahamson, N. A., and Silva, W. J. (1997). ''Empirical response spectral attenuation relations for shallow crustal earthquakes.'' *Seismol. Res. Lett.*, 68(1), 94–127.

American Society for Testing and Materials (ASTM). (2002). *Standard test methods for laboratory compaction characteristics of soil using modified effort*, ASTM International, West Conshohocken, Pa.

Arias, A. (1970). ''A measure of earthquake intensity.'' *Seismic design for nuclear power plants*, R. J. Hansen, ed., MIT, Cambridge, Mass., 438–483.

Cressie, N. A. C. (1991). *Statistics for spatial data*, Wiley, New York.

Houston, S. L. (1992). ''Partial wetting collapse predictions.'' *Proc., 7th Conf. on Expansive Soils*, Texas Tech University Press, Lubbock, Tex., 1, 302–306.

Hudson, M., Idriss, I. M., and Beikae, M. (1994). ''*QUAD4M*: A computer program to evaluate the seismic response of soil structures using finite element procedures and incorporating a compliant base,'' Center for Geotechnical Modeling, Univ. of California, Davis, Calif.

Idriss, I. M., and Sun, J. I. (1991). ''User's manual for *SHAKE91*: A computer program for conducting equivalent linear seismic response analyses of horizontally layered soil deposits,'' Center for Geotechnical Modeling, Univ. of California, Davis, Calif.

Liu, A. H., Stewart, J. P., Abrahamson, N. A., and Moriwaki, Y. (2001). ''Equivalent number of uniform stress cycles for soil liquefaction analysis.'' *J. Geotech. Geoenviron. Eng.*, 127(12), 1017–1026.

Pyke, R., Seed, H. B., and Chan, C. K. (1975). ''Settlement of sands under multidirectional shaking.'' *J. Geotech. Eng.*, 101(4), 379–398.

Rathje, E. M., Abrahamson, N. A., and Bray, J. D. (1998). ''Simplified frequency content estimates of earthquake ground motions.'' *J. Geotech. Geoenviron. Eng.*, 124(2), 150–159.

Rodriguez-Marek, A., Bray, J. D., and Abrahamson, N. A. (2001). ''An empirical geotechnical seismic site response procedure.'' *Earthquake Spectra*, 17(1), 65–87.

Seed, H. B. (1967). ''Soil stability problems caused by earthquakes.'' Soil Mechanics and Bituminous Materials Research Laboratory, Univ. of California, Berkeley, Calif.

Seed, H. B., and Idriss, I. M. (1970). ''Soil moduli and damping factors for dynamic response analysis.'' *Rep. No. UCB/EERC-70/10*, Univ. of California, Berkeley, Calif.

Siddharthan, R. V., and El-Gamal, M. (1996). ''Earthquake induced ground settlements of bridge abutment fills.'' Analysis and design of retaining structures, *Geotechnical Special Publication No. 60*, ASCE, New York, 100–123.

Silva, W. (1986). ''Soil response to earthquake ground motion.'' *Rep. No. RP2556-07*, Electrical Power Research Institute, Palo Alto, Calif.

Silva, W. J., Darragh, R. B., Stark, C., Wong, I., Stepp, J. C., Schneider, J. F., and Chiou, S.-J. (1990). ''A methodology to estimate design response spectra in the near-source region of large earthquakes using the band-limited-white noise ground motion model.'' *Proc., 4th U.S. National Conf. on Earthquake Engineering*, Earthquake Engineering Research Institute, El Cerrito, Calif. 1, 487–494.

Silver, M. L., and Seed, H. B. (1971). ''Volume changes in sands during cyclic loading.'' *J. Soil Mech. Found. Div.*, 97(9), 1171–1182.

Slosson, J. E. (1975). ''Chapter 19: Effects of the earthquake on residential areas.'' *San Fernando, California, Earthquake of 9 February 1971, Bulletin No. 196*, California Division of Mines and Geology, Sacramento Calif.

Stewart, J. P., Smith, P. M., Whang, D. H., and Bray, J. D. (2002). ''Documentation and analysis of field case histories of seismic compression during the 1994 Northridge, California, earthquake.'' *Rep. No. PEER-2002/09*, Pacific Earthquake Engineering Research Center, Univ. of California, Berkeley, Calif.

Stewart, J. P., Bray, J. D., McMahon, D. J., Smith, P. M., and Kropp, A. L. (2001). ''Seismic performance of hillside fills.'' *J. Geotech. Geoenviron. Eng.*, 127(11), 905–919.

Tokimatsu, K., and Seed, H. B. (1987). ''Evaluation of settlements in sands due to earthquake shaking.'' *J. Geotech. Eng.*, 113(8), 861–878.

Toro, G. R. (1997). ''Probabilistic models of shear-wave velocity profiles at the Savannah River site, South Carolina.'' *Rep. to Pacific Engineering and Analysis*, El Cerrito, Calif.

Vucetic, M. (1994). ''Cyclic threshold shear strains in soils.'' *J. Geotech. Eng.*, 120(12), 2208–2228.

Vucetic, M., and Dobry, R. (1991). ''Effect of soil plasticity on cyclic response.'' *J. Geotech. Eng.*, 117(1), 89–107.

Wald, D. J., and Heaton, T. H. (1994). ''A dislocation model of the 1994 Northridge, California, earthquake determined from strong ground motions.'' *Open-File Rep. No. 94-278*, U.S. Geological Survey, Pasadena, Calif.

Whang, D. H., Stewart, J. P., and Bray, J. D. (2004). ''Effect of compaction conditions on the seismic compression of compacted fill soils.'' *Geotech. Test. J.*, in press.